

# Thin Film Diblock Copolymers in Electric Field: Transition from Perpendicular to Parallel Lamellae

Yoav Tsori and David Andelman

School of Physics and Astronomy

Raymond and Beverly Sackler Faculty of Exact Sciences

Tel Aviv University, 69978 Ramat Aviv, Israel

29/9/01

## Abstract

We examine the alignment of thin film diblock copolymers subject to a perpendicular electric field. Two regimes are considered separately: weak segregation and strong segregation. For weakly segregated blocks, below a critical value of the field,  $E_c$ , surface interactions stabilize stacking of lamellae in a direction parallel to the surfaces. Above the critical field, a first-order phase transition occurs when lamellae in a direction perpendicular to the confining surfaces (and parallel to the field) become stable. The film morphology is then a superposition of parallel and perpendicular lamellae. In contrast to Helfrich-Hurault instability for smectic liquid crystals, the mode that gets critical first has the natural lamellar periodicity. In addition, undulations of adjacent inter-material dividing surfaces are out-of-phase with each other. For diblock copolymers in the strong segregation regime, we find two critical fields  $E_1$  and  $E_2 > E_1$ . As the field is increased from zero above  $E_1$ , the region in the middle of the film develops an orientation perpendicular to the walls, while the surface regions still have parallel lamellae. When the field is increased above  $E_2$  the perpendicular alignment spans the whole film.

# 1 Introduction

Diblock copolymers are known to self-assemble into a variety of ordered structures, with a length scale ranging from nanometers to micrometers. These phases have potential applications in nanolithographic templates,<sup>[1]</sup> waveguides<sup>[2]</sup> and dielectric mirrors.<sup>[3]</sup> The length scale and morphology in the melt can easily be adjusted by controlling the fraction  $f = N_A/N$  of A monomers in an A/B chain of  $N = N_A + N_B$  monomers, and the temperature  $T$ .<sup>[4, 5, 6]</sup>

In experiments one often encounters samples in the lamellar phase (made up of alternating planar A- and B-rich domains) in which the melt is only partially ordered. Ordered microdomains, or grains (typical size in the micrometer range), with grain boundaries between them are defects that cost energy. In order to anneal these defects, and to create a perfect alignment of the lamellae, several techniques have been used. In the bulk, mechanical shear proved to be a successful technique. Alignment by application of an electric field<sup>[7, 8, 9, 10]</sup> is also possible, but for macroscopic samples it requires high voltage difference between the two bounding electrodes. Nevertheless, this technique is especially suitable for thin films, because the thickness involved makes the required large fields (typically  $20 - 30 \text{ V}/\mu\text{m}$ ) accessible.

We consider in this paper thin films of lamellar diblock copolymers, under the influence of a perpendicular electric field. Initially, the lamellae are parallel to the confining surfaces, because of preferential short-range interactions with the surfaces. In section 2 we consider diblock copolymers in the weak segregation regime. We show in section 3 that electric field applied perpendicular to the surfaces can cause the melt to transform from a parallel to a perpendicular orientation through a first-order phase transition. The critical field  $E_c$  for this transition is caused by a competition between the electric field and interfacial interactions. In section 4 we investigate the thin-film alignment for diblocks in the strong segregation regime. In this regime, the surface correlations are finite, and thus the range of parallel ordering induced by the surfaces is finite as well. We give the transitions between parallel, perpendicular and mixed lamellae in terms of the system parameters, using a phenomenological model. In both weak and strong segregation regimes, large distortions are present in the copolymer film, and these could be observed in experiments.

## 2 Weakly segregated lamellae

The copolymer order parameter  $\phi(\mathbf{r}) = \phi_A(\mathbf{r}) - f$  is the deviation of the A monomer local volume fraction from its average  $f$ . Above the order-disorder transition (ODT) temperature, the melt is in the disordered, homogeneous state, with  $\phi(\mathbf{r}) = 0$ . As the temperature is reduced below the ODT temperature, the system goes through a first order phase-transition to the lamellar phase. Close to the ODT temperature and in the single-mode approximation, the block copolymer (BCP) order parameter is then given by

$$\phi(\mathbf{r}) = \phi_L \cos(\mathbf{q}_0 \cdot \mathbf{r}) \quad (1)$$

where  $d_0 = 2\pi/q_0$  is the period of lamellar modulations, and  $\phi_L$  is their amplitude (to be determined later).

Consider a copolymer melt below the ODT confined by two flat parallel surfaces at  $y = \pm \frac{1}{2}L$ , as in Fig. 1. The surfaces reduce chain entropy, but also chemically interact with the polymers. The difference in the A and B-block surface interactions  $\sigma_{AS}$  and  $\sigma_{BS}$  defines the parameter  $\sigma$ ,

$$\sigma = \sigma_{AS} - \sigma_{BS} \quad (2)$$

In general,  $\sigma$  can be different for the two surfaces, and hence  $\sigma^+$  is defined on the  $y = \frac{1}{2}L$  surface and  $\sigma^-$  is defined for  $y = -\frac{1}{2}L$ . The surface interaction,  $F_s$ , can be written as an integral over the bounding surfaces (in units of  $k_B T$ )

$$\mathcal{F}_s = \int \{ \sigma^- \phi^- + \sigma^+ \phi^+ \} dx dz \quad (3)$$

where  $\phi^- = \phi(y = -\frac{1}{2}L)$  and  $\phi^+ = \phi(y = \frac{1}{2}L)$ . Terms which do not depend on the copolymer order parameter are not important to subsequent calculations, and were dropped out. The interaction is short-range, localized at the surfaces. A positive  $\sigma^\pm > 0$  induces adsorption of the B monomers ( $\phi^\pm < 0$ ), and  $\sigma^\pm < 0$  the adsorption of the A monomers ( $\phi^\pm > 0$ ). We restrict ourselves to homogeneous surfaces, for which  $\sigma^\pm$  are taken to be constants over each of the two surfaces.

First let us consider a BCP film without an external electric field. We have already considered this case in a previous publication,<sup>[11]</sup> and briefly review here the BCP behavior. If the surface affinities  $\sigma^\pm$  are sufficiently large, the lamellae will order in a parallel arrangement. These lamellae stretch or compress, increasing the bulk free energy, in order to decrease interfacial

energy. We use below an adaptation of the strong stretching approximation used by Turner <sup>[12]</sup> and Walton *et al.* <sup>[13]</sup> to describe these lamellae. The lamellar period is  $d_0 = 2\pi/q_0$  and  $m$  is the closest integer to  $L/d_0$ . Depending on the values of  $\sigma^\pm$ , an integer ( $n = m$ ) or half integer ( $n = m + 1/2$ ) number of lamellae exist between the two surfaces. In the former case the ordering is symmetric (the same type of monomers wet both surfaces), while in the latter it is asymmetric (A monomers wet one surface, whereas B monomers wet the other surface). The parallel lamellae are described by an order parameter  $\phi_\parallel$  given by <sup>[11]</sup>

$$\phi_\parallel(y) = \pm\phi_L \cos[q_\parallel(y + \frac{1}{2}L)] \quad (4)$$

The wavenumber is  $q_\parallel = 2\pi n/L$ , and the choice of  $\pm$  sign in eq 4 is such that the interfacial interactions, eq 3, are minimized. The amplitude of sinusoidal modulations  $\phi_L$  is equal to the amplitude of density modulations in a bulk system, and is given below [eq 13].

We consider now the case where an electric field is turned on, in a direction which is perpendicular to the surfaces ( $y$ -axis in Fig. 1). Under conditions of constant voltage difference across the electrodes situated at the two bounding surfaces, minimum free energy is obtained by maximizing the capacitance. Noting that the A- and B-monomers (blocks) have different dielectric constants, the effect of the electric field is to align the BCP layers parallel to the field, i.e. perpendicular to the surfaces. At a certain field strength,  $E_c$ , this tendency balances the preference for parallel lamellae as induced by the surfaces. Further increase of  $E$  above the critical value  $E_c$  gives rise to a perpendicular lamellar ordering.

Close to the ODT, the copolymer ordering is weak, and the energetic cost of compressing or bending the lamellae is small. In this regime the inter-material dividing surface (IMDS) of the lamellar phase, given by the requirement  $\phi(\mathbf{r}) = 0$ , can be substantially perturbed from its flat state. This reasoning leads us to the following superposition ansatz. For zero electric field  $E$ , interfacial interactions orient the lamellae in a parallel orientation. The order parameter is then given by  $\phi(\mathbf{r}) = w(E = 0)\phi_\parallel(y)$ . The dimensionless amplitude  $w > 0$  is determined by the strength of interfacial interactions, and can be larger than unity if  $\sigma^\pm$  are sufficiently large. Namely the surface induced order can be stronger than in the bulk. Upon increase of the electric field, the function  $w(E)$  of this parallel state diminishes, while the function  $g(E)$  of perpendicular lamellae (parallel to the electric field) increases. This can be modeled by using the superposition ansatz for the

order parameter  $\phi(\mathbf{r}, E)$  in the presence of the field  $E$ :

$$\phi(\mathbf{r}, E) = w(E)\phi_{\parallel}(\mathbf{r}) + g(E)\phi_{\perp}(\mathbf{r}) \quad (5)$$

The order parameter of the perpendicular lamellae is  $\phi_{\perp}(x)$ . It depends only on the wavenumber  $q_{\perp}$ , and is given in the single-mode approximation (weak segregation) by

$$\phi_{\perp}(\mathbf{r}) = \phi_{\perp}(x) = \phi_L \cos(q_{\perp}x) \quad (6)$$

The wavenumber  $q_{\perp}$  is yet to be determined. Without the electric field,  $E = 0$ , the amplitude of perpendicular modulations vanishes,  $g = 0$ . As the limit  $E \rightarrow \infty$  is approached, the effect of the confining surfaces becomes negligible, and the BCP ordering is given by the bulk perpendicular lamellae  $\phi_{\perp}$  ( $g = 1$ ). Hence, the weight amplitudes  $w(E)$  and  $g(E)$  satisfy the following limits as function of  $E$ :

$$g(E = 0) = 0, \quad g(E = \infty) = 1 \quad (7)$$

$$w(E = 0) = \text{const}, \quad w(E = \infty) = 0 \quad (8)$$

In order to get explicit expression for the weight functions  $w$  and  $g$  we need to consider a specific model. The free energy we use in this section is applicable to the weak segregation regime, and is given by  $\mathcal{F} = \mathcal{F}_b + \mathcal{F}_s$ ,<sup>[14, 15, 16]</sup> with  $\mathcal{F}_s$  from eq 3, and  $\mathcal{F}_b$  being the bulk contribution. This part of the free energy has a polymer (non-electrostatic) and electrostatic contributions (in units of  $k_B T$ ),

$$\mathcal{F}_b = \mathcal{F}_p + \mathcal{F}_{\text{el}} \quad (9)$$

The polymer part have been used several times in the past:<sup>[14, 15, 16, 17, 18]</sup>

$$\mathcal{F}_p = \int \left\{ \frac{1}{2} \tau \phi^2 + \frac{1}{2} h (q_0^2 \phi + \nabla^2 \phi)^2 + \frac{u}{24} \phi^4 \right\} d^3 r \quad (10)$$

The parameters in 10 are given by

$$q_0 \simeq 1.95/R_g \ ; \ h = 3\rho c^2 R_g^2 / 2q_0^2 \quad (11)$$

$$\chi_c \simeq 10.49/N \ ; \ \tau = 2\rho N (\chi_c - \chi) \quad (12)$$

Denoting  $b$  as the monomer size, the radius of gyration for Gaussian chains is  $R_g^2 \simeq \frac{1}{6} N b^2$ . The polymerization index is  $N$ , the chain density of an incompressible melt is  $\rho = 1/N b^3$ , and  $\chi$  is the Flory parameter. The amplitude  $\phi_L$  in the parallel and perpendicular states is

$$\phi_L^2 = -8\tau/u \ , \quad \tau < 0 \quad (13)$$

as is obtained by inserting eq 1 in  $\mathcal{F}_p$  of eq 10 and minimization with respect to  $\phi_L$ . The dimensionless ratio  $u/\rho$  and  $c$  are of order unity, and are taken to be equal to one in the remaining of the paper,  $u/\rho = c = 1$ .

The electrostatic contribution in units of  $k_B T$  is [7, 19]

$$\mathcal{F}_{\text{el}} = \beta \int (\hat{\mathbf{q}} \cdot \mathbf{E})^2 \phi_{\mathbf{q}} \phi_{-\mathbf{q}} d^3 q \quad (14)$$

$$\beta = \frac{(\varepsilon_A - \varepsilon_B)^2}{16(2\pi)^4 k_B T \langle \varepsilon \rangle} \quad (15)$$

Here  $\phi_{\mathbf{q}}$  is the Fourier transform of  $\phi(\mathbf{r})$ :  $\phi(\mathbf{r}) = \int \phi_{\mathbf{q}} \exp(i\mathbf{q} \cdot \mathbf{r}) d\mathbf{q}$ , and  $\hat{\mathbf{q}} = \mathbf{q}/q$ . Copolymer modulations with a non-vanishing component of the wavenumber  $\mathbf{q}$  along the electric field, have a positive contribution to the free energy. In other words, there is a free energy penalty for having dielectric interfaces in a direction perpendicular to the electric field. In eq 15,  $\varepsilon_A$  and  $\varepsilon_B$  are the dielectric constants of the pure A and B-blocks, respectively, [7, 8] and  $\langle \varepsilon \rangle$  is the material average dielectric constant for the BCP film,

$$\langle \varepsilon \rangle = f\varepsilon_A + (1 - f)\varepsilon_B \quad (16)$$

Throughout the remaining of this paper we will focus only on symmetric melts ( $f = \frac{1}{2}$ ), having an average dielectric constant  $\langle \varepsilon \rangle = \frac{1}{2}(\varepsilon_A + \varepsilon_B)$ . For small concentration variations, valid in the weak segregation regime,  $\varepsilon$  varies linearly with the local copolymer composition  $\phi$ ,

$$\begin{aligned} \varepsilon(\phi) &= \left(\frac{1}{2} + \phi\right)\varepsilon_A + \left(\frac{1}{2} - \phi\right)\varepsilon_B \\ &= \langle \varepsilon \rangle + (\varepsilon_A - \varepsilon_B)\phi \end{aligned} \quad (17)$$

It is possible to perform the spatial integration in eqs. 3, 10 and 14, yielding the free energy per unit volume  $F = F_p + F_{\text{el}} + F_s$  for a general order parameter  $\phi(\mathbf{r})$ , eq 5:

$$\begin{aligned} F &= \frac{1}{4}\phi_L^2 [(\tau + C_{\parallel})w^2 + (\tau + C_{\perp})g^2] \\ &+ \frac{u\phi_L^4}{64}(w^4 + g^4) + \frac{u\phi_L^4}{16}w^2g^2 + \frac{w\Sigma}{L} \end{aligned} \quad (18)$$

The quantities  $C_{\parallel}$  and  $C_{\perp}$  are positive and given by

$$C_{\parallel} = h(q_0^2 - q_{\parallel}^2)^2 + 2\beta E^2 \quad (19)$$

$$C_{\perp} = h(q_0^2 - q_{\perp}^2)^2 \quad (20)$$

$\Sigma = \pm\phi_L\sigma^- \pm \phi_L\sigma^+$  is related to the interfacial free energy, and is negative. The  $\pm$  sign is determined from the  $\pm$  sign of the order parameter in eq 4. The free energies  $F_{\parallel}$  and  $F_{\perp}$  of the parallel and perpendicular states are given as limiting cases

$$F_{\parallel} = F(w, g = 0) = \frac{1}{4}\phi_L^2(\tau + C_{\parallel})w^2 + \frac{u\phi_L^4}{64}w^4 + \frac{w\Sigma}{L} \quad (21)$$

$$F_{\perp} = F(w = 0, g = 1) = \frac{1}{4}\phi_L^2(\tau + C_{\perp}) + \frac{u\phi_L^4}{64} \quad (22)$$

As discussed in the introduction, we concentrate on the interesting case where in the absence of electric field, the BCP has a parallel ordering given by  $\phi = w\phi_{\parallel}$  (with some weight  $w$ ). This is equivalent to saying that there exist  $w$  such that  $F_{\parallel}(E = 0) < F_{\perp}(E = 0)$ . By inserting  $E = 0$  and  $q_{\perp} = q_0$  in eqs. 21 and 22 we get that in this case

$$\frac{1}{4}\phi_L^2(\tau + C_{\parallel})w^2 + \frac{u\phi_L^4}{64}w^4 + \frac{w\Sigma}{L} < -\tau^2/u \quad (23)$$

Therefore, the free energy of the parallel lamellae is expected to be lower than the free energy of the perpendicular lamellae. This assumption is valid for strong enough interfacial interactions,  $\Sigma$ . In the next section we proceed to find the weight functions  $w(E)$  and  $g(E)$  for any  $E > 0$ .

### 3 Results of the weak segregation model

The free energy eq 18 is minimized with respect to  $w$  and  $g$  to yield two coupled algebraic equations:

$$(\tau + C_{\perp})g - \tau g^3 - 2\tau w^2 g = 0 \quad (24)$$

$$(\tau + C_{\parallel})w - \tau w^3 - 2\tau g^2 w + 2\Sigma/L\phi_L^2 = 0 \quad (25)$$

These equations are analyzed separately for small and large electric fields.

#### (i) Small electric fields: $E < E_c$ .

For zero electric field, the lamellae are in their parallel state, namely  $g = 0$ . The solution with  $g(E) = 0$  and  $w(E) \neq 0$  [in eqs. 24 and 25] corresponds to the minimum of the free energy if  $E$  is below a certain threshold value  $E_c$ ,

which is to be determined later. Denoting  $g_<(E)$  and  $w_<(E)$  as the weight amplitudes for electric fields  $E < E_c$ , they satisfy the following equations:

$$g_<(E) = 0 \quad (26)$$

$$(\tau + C_{\parallel})w_<(E) - \tau w_<^3(E) + 2\Sigma/L\phi_L^2 = 0 \quad (27)$$

**(ii) Large electric fields:  $E > E_c$ .**

There is a solution to eqs. 24 and 25 with perpendicular lamellae, namely with a nonzero  $g(E)$ . This solution gives the minimum of the free energy above a critical field,  $E > E_c$ . The weight amplitudes  $g_>(E)$  and  $w_>(E)$  are then given by:

$$g_>^2(E) = \frac{\tau + C_{\perp}}{\tau} - 2w_>^2(E) \geq 0 \quad (28)$$

$$(-\tau + C_{\parallel} - 2C_{\perp})w_>(E) + 3\tau w_>^3(E) + 2\Sigma/L\phi_L^2 = 0 \quad (29)$$

The above solution is valid provided that  $w_>$  is small enough, as given by the inequality

$$w_>^2(E) \leq \frac{1}{2} + \frac{C_{\perp}}{2\tau} \leq \frac{1}{2} \quad (30)$$

Since  $w(E)$  is a decreasing function, from eq 20 we see that increasing the electric field  $E$  from zero, the natural mode of the perpendicular state,  $q_{\perp} = q_0$ , is the first to become critical. Namely, the inequality above is obeyed first by the  $q_{\perp} = q_0$  mode, and only later by other  $q$ -modes. For this reason we assume from this point on that  $q_{\perp} = q_0$ , yielding  $C_{\perp} = 0$  and  $g_>^2(E) = 1 - 2w_>^2(E)$ . Thus, BCP modulations in a direction parallel to the surfaces have the bulk (free) periodicity  $d_0$ .

Equation 29 is a cubic equation for  $w_>$  and has an analytical solution. It is convenient to express the solution via a parameter  $\theta$  defined as

$$\cos[\theta(E)] \equiv -\frac{\Sigma/L\phi_L^2}{3\tau} \left( \frac{\tau - C_{\parallel}}{9\tau} \right)^{-3/2} < 0 \quad (31)$$

and take it to be in the range  $\pi < \theta < \frac{3}{2}\pi$ . Recalling that  $\Sigma$  and  $\tau$  are negative, the solution  $w_>$  to eq 29 is then simply given by

$$w_>(E) = 2\sqrt{\frac{\tau - C_{\parallel}}{9\tau}} \cos\left(\frac{1}{3}\theta\right) \quad (32)$$

Curves of  $g(E)$  and  $w(E)$  are shown in Fig. 2 within the assumption  $q_{\perp} = q_0$ . For zero electric field, the film has parallel lamellae,  $g(0) = 0$ .



With increasing electric field  $E$ , the amplitude  $w_<(E)$  of parallel lamellae decreases monotonically, as is given by eq 27. At the critical field,  $E = E_c$ , there is a first-order phase transition, and perpendicular lamellae appear. The weight amplitudes  $w(E)$  and  $g(E)$  are discontinuous, the jump in their values,  $\Delta w$  and  $\Delta g$ , is determined by the degree of segregation  $N\chi$ , inter-surface separation  $L$  and surface parameters  $\sigma^\pm$ . Further increase of the electric field causes  $g(E)$  to increase while  $w(E)$  decreases. For very large electric fields,  $E \rightarrow \infty$ , the perpendicular state saturates to its value  $g = 1$ , and parallel lamellae completely disappear,  $w = 0$ .

The critical field  $E_c$  is determined by the condition

$$F(w_<, g_<) = F(w_>, g_>) \quad (33)$$

where  $F$  is taken from eq 18. Namely, it is the field where the two values of the free energy cross. The critical field  $E_c$  as a function of surface separation  $L$  is shown in Fig. 3 a for weak segregations ( $N\chi = 11$ ). As the surface separation  $L$  increases (or the interfacial interaction  $\Sigma$  decreases),  $E_c$  decreases with typical oscillations of period  $d_0$ . These oscillations are caused by the frustration occurring when the surface separation is incommensurate with the lamellar period. Figure. 3 b shows a log-log plot of the same curve. The dashed line shows a fit to a  $E_c \sim L^{-1/2}$  scaling. This scaling can be obtained by balancing the surface tension  $\sigma$  (independent of  $L$ ), with the electrostatic contribution  $\sim LE_c^2$ . There is a good fit between this  $L^{-1/2}$  line and the position of peaks, as expected for unstrained films.<sup>[20]</sup> However, for frustrated films the deviation from  $E_c \sim L^{-1/2}$  becomes increasingly important as the surface separation  $L$  is reduced below roughly  $6d_0$  for the parameters used.

We define  $w_<^c$  as the value of  $w$  just before the transition ( $E \uparrow E_c$ ), and  $w_>^c$  the value after the transition ( $E \downarrow E_c$ ), and similarly for  $g$ . The jump in the weight amplitudes  $\Delta w$  and  $\Delta g$  is

$$\Delta w = |w_>^c - w_<^c| \quad (34)$$

$$\Delta g = g_>^c - g_<^c = g_>^c \quad (35)$$

These quantities are plotted as a function of surface separation  $L$  in Fig. 3 c, for the same parameters as in Fig. 3 a. As  $L$  increases, the critical field  $E_c$  decreases, the jump in  $w$  and  $g$  gets larger, and the transition from parallel to perpendicular lamellae becomes more abrupt.

In Fig. 4 we show how the film changes its orientation and morphology as the electric field increases. In part a we show a contour plot of the copolymer order parameter  $\phi = w(E)\phi_\parallel + g(E)\phi_\perp$ , for  $E < E_c$ , but only slightly

below it. The ordering in the film is parallel to the surfaces, as  $g(E) \equiv 0$ . In part b the field is increased above its threshold value  $E_c$ , and the undulations created by the appearance of the perpendicular state are prominent. In contrast to the classical Helfrich-Hurault undulations [21] calculated for smectic and cholesteric liquid crystals, here the lateral wavelength is finite, and is equal to the free periodicity  $d_0$ . In addition, the modulations of the adjacent IMDS, given by  $\phi(\mathbf{r}) = 0$ , are shown in part c to be out-of-phase with each other. Although the perpendicular ordering may be very strong, some parallel ordering is still present (finite  $w > 0$ ). As the electric field is further increased, there is only little reminiscence of the parallel ordering, and the perpendicular lamellae are nearly perfect. This can be seen in Fig. 4 d, where we choose  $E = 4E_c$ .

## 4 Strongly segregated lamellae

In this section we consider the same alignment phenomenon under an electric field as in the previous section, but the BCP melt is assumed to be in the strong segregation limit, i.e.  $N\chi \gg 10.5$ . In this regime the lamellae are not easily deformed, and the effect of the surface field is important only close to the confining walls, in contrast to the long-range ordering in the weak segregation.

### 4.1 Unstrained films

For simplicity, we discuss first the alignment phenomenon ignoring the effect of incommensurability between the film thickness  $L$  and the free lamellar period  $d_0$ . In the following section we consider strained films as well. For simplicity, we also assume that the two walls are chemically identical, and preferring the B monomers:  $\sigma_{AS} > \sigma_{BS}$ ,  $\sigma^\pm > 0$ . For sufficiently strong  $E$  we expect to nucleate a region in the middle of the film with lamellae perpendicular to the walls, as is shown schematically in Fig. 5. Hence two regions of a “T-junction” morphology will exist in the film, in the vicinity of the bounding surfaces.

We denote the size of the region that is perpendicular to the surfaces by  $l$ . If  $l = 0$  the film has only parallel ordering, while for  $l = L$  the perpendicular ordering spans the whole film. The free energies per unit area,  $F_\parallel$  and  $F_\perp$ ,

for these two extreme cases are:

$$F_{\parallel} = LF_p + 2\sigma_{\text{BS}} - \lambda_{\parallel}LE^2 \quad (36)$$

$$F_{\perp} = LF_p + \sigma_{\text{AS}} + \sigma_{\text{BS}} - \lambda_{\perp}LE^2 \quad (37)$$

$F_p$  is the polymer free energy per unit volume of a BCP in the lamellar phase, and in the above we have used

$$\begin{aligned} \lambda_{\parallel} &= \frac{1}{16\pi} \left[ \frac{4\varepsilon_A\varepsilon_B}{\varepsilon_A + \varepsilon_B} - 2 \right] \\ \lambda_{\perp} &= \frac{1}{16\pi} [\varepsilon_A + \varepsilon_B - 2] \end{aligned} \quad (38)$$

Note that  $\lambda_{\perp} > \lambda_{\parallel}$ , meaning that  $-\lambda_{\perp}E^2 < -\lambda_{\parallel}E^2$ , and the perpendicular state is favored for  $E \rightarrow \infty$ .

Let us focus on the mixed state as is illustrated in Fig. 5. For intermediate values of  $l$ ,  $0 < l < L$ , there are two surface regions of parallel orientation and a central region of perpendicular orientations. The free energy of this mixed state (per unit area)  $F_M$  is:

$$F_M = LF_p + 2\sigma_{\text{BS}} + 2\gamma_T - \lambda_{\perp}lE^2 - \lambda_{\parallel}(L-l)E^2 \quad (39)$$

A positive energy penalty (per unit area)  $\gamma_T$  is associated with each of the two T-junction defects.

The value of the interfacial energies  $\sigma_{\text{AS}}$ ,  $\sigma_{\text{BS}}$  and  $\gamma_T$  must depend on  $l$ . To see this consider, for example,  $L \gg d_0$  and  $l = \frac{1}{2}L$ . In this case  $\gamma_T$  is some constant. But as  $l \rightarrow L$ , the value of  $\gamma_T$  must approach zero, because when  $l = L$  the T-junction does not exist, and the energy associated with it is zero. We denote by  $a$  the cutoff length, which is the characteristic width at which  $\gamma_T$  goes to zero. From the same reason  $\gamma_T$  must also tend to zero as  $l \rightarrow 0$ , with another cutoff length. For simplicity we assume that this cutoff length is also equal to  $a$ . Similarly, the interfacial energies  $\sigma_{\text{AS}}$  and  $\sigma_{\text{BS}}$  tend to zero as  $l \rightarrow L$ , with the same cutoff length. The qualitative forms of these parameters are shown in Fig. 6 a. The smooth monotonic decay to zero at  $l = L$  and  $l = 0$  is only suggestive.  $\gamma_T(l)$  has oscillations with period  $\frac{1}{2}d_0$ .

In principle, one should minimize  $F_M$  with respect to the size of perpendicular domain  $l$ . This generalized (mixed) state would correspond to the parallel state when the minimum is at  $l = 0$ , and to the perpendicular state when the minimum is at  $l = L$ . However, we do not know from a molecular

description how  $\sigma_{AS}$ ,  $\sigma_{BS}$  and  $\gamma_T$  fall off to zero, and therefore use the approximation shown in Fig. 6 b.  $\sigma_{AS}(l) = \sigma_{AS}^0$  and  $\sigma_{BS}(l) = \sigma_{BS}^0$  are constant for  $l < L - a$  and zero for  $l > L - a$ .  $\gamma_T(l) = \gamma_T^0$  is constant in the range  $a < l < L - a$ , and zero otherwise. To make the notation simpler we drop hereafter the superscript zero of  $\sigma_{AS}$ ,  $\sigma_{BS}$  and  $\gamma_T$ .

With the above assumptions, the size  $l$  of a perpendicular domain that minimizes the mixed free energy  $F_M$  is  $l = L - 2a$ , and the free energy at its minimum value is

$$F_M = LF_p + 2\sigma_{AS} + 2\gamma_T - [(L - 2a)\lambda_{\perp} + 2a\lambda_{\parallel}] E^2 \quad (40)$$

Note that the effect of incommensurability between the surface spacing  $L$  and the lamellar period  $d_0$ , appears as undulations in the plot of  $\gamma_T(l)$  (Fig. 6 a), and these undulations are neglected here.

The plot of  $F_{\parallel}$ ,  $F_{\perp}$  and  $F_M$  as a function of electric field strength  $E$  is shown in Fig. 7. Without loss of generality, we assume that  $\sigma_{BS} < \sigma_{AS}$  and the B-polymer is adsorbed at the surfaces in the parallel state. The dimensionless parameter  $\delta$  measuring the difference in A and B-block interfacial interactions is defined as:

$$\delta \equiv \frac{\sigma}{\gamma_T} = \frac{\sigma_{AS} - \sigma_{BS}}{\gamma_T} \quad (41)$$

Based on the value of  $\delta$ , we now discuss two cases:

**(i) Strong surface fields:  $\delta > \delta^*$ .**

If  $\delta$  is larger than a threshold value  $\delta^*$ , given by

$$\delta^* \equiv \frac{2L}{L - 2a} > 2 \quad (42)$$

there are two distinct critical fields  $E_1$  and  $E_2 > E_1$  given by

$$E_1 = \left[ \frac{2\gamma_T}{(L - 2a)(\lambda_{\perp} - \lambda_{\parallel})} \right]^{1/2} \quad (43)$$

$$E_2 = \left[ \frac{\gamma_T(\delta - 2)}{2a(\lambda_{\perp} - \lambda_{\parallel})} \right]^{1/2} \quad (44)$$

The smallest of these fields,  $E_1$ , obtained for  $F_M = F_{\parallel}$ , decays to zero like  $E \propto (L - 2a)^{-1/2}$ . This is the field required to create the T-junction defect in the film. For  $E$  fields in the range  $E_1 < E < E_2$ , the film has a region

of size  $l = L - 2a$  with perpendicular lamellae, while parallel lamellae are localized in a small region of size  $a$  near the two walls. The second field,  $E_2$ , obtained for  $F_M = F_\perp$ , is larger than  $E_1$  and does not depend on surface separation  $L$ . It corresponds to the electric field that is required to destroy the parallel surface layer (of width  $a$ ). Note also the appearance of  $\lambda_\perp - \lambda_\parallel$  in the denominator of the two critical fields. If the dielectric contrast between A and B domains is small, namely  $\varepsilon_A/\varepsilon_B \approx 1$ , then this quantity is small, and the critical fields are large. If, on the other hand,  $\varepsilon_A/\varepsilon_B \gg 1$ , then the critical fields required to achieve mixed and perpendicular lamellae are small.

**(ii) Weak surface fields:  $\delta < \delta^*$ .**

For small values of  $\delta$ , namely  $\delta < \delta^*$ , the free energies  $F_\perp$  and  $F_\parallel$  are always smaller than  $F_M$ . Namely, the mixed state is not a possible minimum of the film free energy. There is only one transition at a critical field  $E_1$  occurring when  $F_\perp$  intersects  $F_\parallel$  (Fig. 7 b). This field is given by:

$$E_1 = \left( \frac{\gamma_T \delta}{L(\lambda_\perp - \lambda_\parallel)} \right)^{1/2} = \left( \frac{\sigma}{L(\lambda_\perp - \lambda_\parallel)} \right)^{1/2} \quad (45)$$

When  $E = E_1$ , a direct transition occurs from a state where the whole film has parallel lamellae to a state where the whole film has perpendicular lamellae without any surface regions.

In Fig. 8 a we show the phase diagram in the plane of electric field  $E$  and  $\delta$ , summarizing the two regimes mentioned above. For small electric fields, the lamellae are in the fully parallel configuration. If  $\delta$  is small, a first-order phase transition to the fully perpendicular state occurs when  $E$  is increased above  $E_1$ , eq 45. If  $\delta$  is large enough, namely  $\delta > \delta^*$ , there are two transitions when the field is increased. In the regime  $E_2 > E > E_1$ , the film is in a mixed state, and layers of thickness  $a$  with parallel lamellae still exist close to the surfaces. As  $E$  is further increased above  $E_2$ , the film has a fully perpendicular state. Note that when  $\delta > \delta^*$ ,  $E_1$  is the field required to initiate the T-junction defect, and so is independent of  $\sigma$ , while  $E_2$  is the field that destroys the surface layer, and therefore  $E_2 \sim (\sigma - 2\gamma_T)^{1/2}$ .

As we have seen, the condition  $\delta > \delta^* = \frac{2L}{L-2a}$  is required for the existence of the mixed state, and hence for the existence of two critical fields  $E_1$  and  $E_2$ . Alternatively, this condition can be viewed as a restriction on the film thickness  $L$ . Therefore, a mixed state exists if

$$L > L^* \equiv \frac{2a\delta}{\delta - 2} = \frac{2a\sigma}{\sigma - 2\gamma_T} \quad (46)$$

Figure 8 b is the phase diagram in the plane of  $E$ - $L$ . For small surface separations,  $L < L^*$ , there is a transition from parallel to perpendicular lamellae at  $E = E_1$ , eq 45. For larger separations,  $L > L^*$ , the mixed state appears at  $E = E_1$  [eq 43]. The transition to a fully perpendicular state occurs at  $E = E_2$ , eq 44. Note that this field is independent of  $L$ . The main difference between this diagram and the one obtained by Pereira and Williams,<sup>[20]</sup> is that we always find the perpendicular state to be favored for large enough electric fields.

## 4.2 Strained films

Strained films occur when the film thickness  $L$  does not match the lamellar period  $d_0$ , namely  $L/d_0$  is not an integer or a half-integer number. The effect of this mismatch, which was neglected in the previous section, is considered below. The strong segregation theory of Turner<sup>[12]</sup> and Walton *et al*<sup>[13]</sup> has been successful in describing confined lamellae, and therefore we use it in this section to include the effect of lamellae frustration, and to modify the free energy  $F_{\parallel}$  from section 4.1. We use the convention that  $m$  is the closest integer to  $L/d_0$ , yielding  $F_{\parallel}$  which is the minimum of  $F_{\parallel}^s$  and  $F_{\parallel}^{as}$ , the symmetric and antisymmetric parallel states free energies, respectively:

$$F_{\parallel}^s = \sigma_{AB} \left[ \left( \frac{L}{d_0} \right)^3 \cdot \frac{1}{n^2} + 2n \right] + 2\sigma_{BS} - \lambda_{\parallel} L E^2$$

for  $n = m$ , symmetric

(47)

$$F_{\parallel}^{as} = \sigma_{AB} \left[ \left( \frac{L}{d_0} \right)^3 \cdot \frac{1}{n^2} + 2n \right] + \sigma_{AS} + \sigma_{BS} - \lambda_{\parallel} L E^2$$

for  $n = m \pm \frac{1}{2}$ , asymmetric

(48)

In the symmetric state, both surfaces are wetted by B monomers, while in the antisymmetric state A monomers adsorb to one surface and B monomers adsorb to the second surface.

In Fig. 9 we present the phase diagrams when the mismatch between  $L$  and  $d_0$  is taken into account, plotted with same parameters as in Fig. 8. For very thin films,  $L < d_0$ , the perpendicular state is favored over the parallel state, even for  $E = 0$ . Apart from this, Fig. 9 a is similar to Fig. 8 a. However,

Fig. 9 b is different than Fig. 8 b. The critical field  $E_1$  separating the parallel state from the other two states has oscillations with period  $d_0$ . This curve is similar to the critical field curve for weakly segregated lamellae, Fig. 3, and also to the curve found by Ashok *et al.* using different parameters.<sup>[22]</sup> Note that from the discussion of unstrained films in section 4.1,  $E_1$  has oscillations around a line which decays as  $E_1 \propto L^{-1}$  for  $L < L^*$ , and as  $E_1 \propto (L - 2a)^{-1}$ , for  $L > L^*$ . The field  $E_2$  separating the mixed state with the perpendicular state remains independent of  $L$ .

## 5 Conclusions

In this paper we study the influence of an applied electric field on the morphology of thin film diblock copolymers. The lamellae are taken to be ordered parallel to the confining surfaces in the absence of an electric field. Strong enough  $E$  fields in the direction perpendicular to the surfaces eventually will orient the lamellae in a perpendicular direction. However, the response of weakly segregated lamellae is different than the response of strongly segregated lamellae. In the former case, the BCP order parameter is obtained as a function of electric field strength  $E$  and other system parameters (such as the degree of segregation  $N\chi$ , strength of interfacial interactions  $\sigma^\pm$  and film thickness  $L$ ). The field applied in the perpendicular direction diminishes the amplitude of the parallel BCP state. Above the critical field,  $E > E_c$ , a first-order phase transition occurs, from the parallel into the perpendicular state.

The first  $q$ -mode which becomes stable in the perpendicular state  $q_\perp$  has a finite periodicity, equal to the bulk spacing  $d_0 = 2\pi/q_0$ . Moreover, modulations of adjacent inter-material dividing surfaces (IMDS) are out-of-phase with each other. This is different than the strong segregation instability studied by Onuki and Fukuda,<sup>[19]</sup> where the slowly varying phase  $\phi = \phi_L \cos[q_0 x + u(y)]$  is used, and the free energy is expanded in small  $u$ . At the onset of instability, they found that adjacent IMDS lines are in-phase with each other. The weak segregation IMDS undulations studied here appear because in this regime it is relatively easy to deform the lamellae. For  $E > E_c$ , parallel and perpendicular lamellae coexist in the film. This superposed state is yet to be verified in experiments.

The critical field  $E_c$  as a function of inter-surface separation  $L$  decays with characteristic oscillations of period  $d_0$ . These oscillations are the result

of lamellar frustration, occurring when the period  $2\pi/q_{\parallel}$  is different than  $d_0$  (while  $q_{\perp}$  is taken always to be equal to  $q_0$ ). The deviation of the critical field  $E_c$  from the  $E_c \sim L^{-1/2}$  scaling (of unstrained films) is important for small surface separations.

The weak segregation treatment we present relies on mean-field theory. It is valid close to the critical point, but not too close where critical fluctuations become important.<sup>[23]</sup> We have ignored the deviations of the inter-material dividing surface from the perfect flat shape that occur near the surfaces. These deviations can be important for small surface separations ( $L \gtrsim d_0$ ), or close to the ODT,<sup>[15, 16]</sup> and should be properly accounted for.

In the second part of the paper we consider BCP film in the strong segregation regime. In contrast to the weak segregation case, here the surface induced ordering has a finite range of length  $a$ . Two critical fields  $E_1$  and  $E_2$  are obtained. For small electric fields,  $E < E_1$ , the film has parallel lamellae. As the field is increased above  $E_1$  but below  $E_2$ , a region of size  $l$  of perpendicular lamellae develops in the middle of the film, provided that the parameter  $\delta$  is large enough,  $\delta > \delta^*$ . In this mixed state, a layer of parallel lamellae of thickness equal to the cutoff length  $a$  still persists close to the surfaces. When  $E > E_2$  the system is in the perpendicular state.

The phase diagrams in the  $E$ - $\delta$  plane and in the  $E$ - $L$  are given in Fig. 8. A direct transition from a parallel to a perpendicular state is realized for small  $\delta$ ,  $\delta < \delta^*$ , as is given by eq 42. For large  $\delta > \delta^*$  there is a transition from parallel to mixed lamellae at  $E = E_1$  [eq 43] and from mixed to perpendicular lamellae at  $E = E_2$  [eq 44]. These diagrams do not take into the frustration effects caused by a mismatch between the wall separation and the natural lamellar periodicity in the bulk. In this respect, they are qualitatively applicable to non-polymeric systems such as ferrosmelectics in magnetic fields,<sup>[24]</sup> and to BCP in the hexagonal phase, as investigated experimentally.<sup>[10]</sup> The difference between the hexagonal and lamellar phases is in the value of  $\lambda_{\parallel}$ ,  $\lambda_{\perp}$ , and in different numerical coefficients in eqs. 36, 37 and 40. These modifications only change the critical fields  $E_1$  and  $E_2$  by a numerical factor, but do not alter the phase behavior. Indeed, two critical fields, between which a regime of mixed state exists, have been found experimentally.<sup>[10]</sup> The threshold field for transition from the mixed to the fully perpendicular state was observed to be independent of  $L$ , as is calculated by us and shown in Fig. 8 b and Fig. 9 b.

When the surface separation  $L$  is not an integer or half integer number of



the bulk lamellar period  $d_0$ , the phase diagrams are given by Fig. 9. While in the  $E$ - $\delta$  plane the behavior is only slightly changed, in the  $E$ - $L$  plane the border of the parallel state has prominent oscillations with period  $d_0$ . Finally, have not considered the copolymer density undulations as was done by Onuki and Fukuda.<sup>[19]</sup> These might change the boundary lines between the parallel, perpendicular and mixed phases.

We predict a dependence of the transition field on the film thickness which will be interesting to verify in experiment. The energy penalty  $\gamma_T$  of the T-junction created in the film, the width  $a$  of the parallel layer, as well as the difference in interfacial energies of the two blocks,  $\sigma = \sigma_{AS} - \sigma_{BS}$ , can be deduced in experiment from the measured values of  $E_1$  and  $E_2$  using eqs. 41, 43 and 44.

## Acknowledgments

We would like to thank J. DeRouchey, M. Doi, R. Rosensweig, M. Schick and T. Taniguchi for fruitful discussions. Partial support from the U.S.-Israel Binational Foundation (B.S.F.) under grant No. 98-00429 and the Israel Science Foundation founded by the Israel Academy of Sciences and Humanities — centers of Excellence Program is gratefully acknowledged.

## References

- [1] Park, M.; Harrison, C.; Chaikin, P. M.; Register, R. A.; Adamson, D. H. *Science* **1997**, *276*, 1401.
- [2] Ibanescu, M.; Fink, Y.; Fan, S.; Thomas, E. L.; Joannopoulos, J. D. *Science* **2000**, *289*, 415.
- [3] Fink, Y.; Winn, J. N.; Fan, S.; Chen, C.; Michel, J.; Joannopoulos, J. D.; Thomas, E. L. *Science* **1998**, *282*, 1679. Urbas, A.; Sharp, R.; Fink, Y.; Thomas, E. L.; Xenidou, M.; Fetters, L. J. *Adv. Matter.* **2000**, *12*, 812.
- [4] Leibler, L. *Macromolecules* **1980**, *13*, 1602.
- [5] Ohta, T; Kawasaki, K. *Macromolecules* **1986**, *19*, 2621.

- [6] Bates, F. S.; Fredrickson, G. H. *Annu. Rev. Phys. Chem.* **1990**, *41*, 525 (1990).
- [7] Amundson, K.; Helfand, E.; Quan, X.; Hudson, S. D. *Macromolecules* **1993**, *26*, 2698.
- [8] Amundson, K.; Helfand, E.; Quan, X. *Macromolecules* **1994**, *27*, 6559.
- [9] Morkved, T.; Lu, M.; Urbas, A. M.; Ehrichs, E. E.; Jaeger, H. M.; Mansky, P.; Russell, T. P. *Science* **1996**, *273*, 931.
- [10] Thurn-Albrecht, T.; DeRouchey, J.; Russell, T. P. *Macromolecules* **2000**, *33*, 3250.
- [11] Tsori Y.; Andelman, D. *Eur. Phys. J. E* **2001**, *5*, 605.
- [12] Turner, M. S. *Phys. Rev. Lett.* **1992**, *69*, 1788.
- [13] Walton, D. G.; Kellogg, G. J.; Mayes, A. M.; Lambooy, P.; Russell, T. P. *Macromolecules* **1994**, *27*, 6225.
- [14] Fredrickson, G. H.; Helfand, E. *J. Chem. Phys.* **1987**, *87*, 697.
- [15] Tsori, Y.; Andelman, D. *Europhys. Lett.* **2001**, *53*, 722.
- [16] Tsori, Y.; Andelman, D. *Macromolecules* **2001**, *34*, 2719.
- [17] Swift, J.; Hohenberg, P. C. *Phys. Rev. A* **1977**, *15*, 319.
- [18] Chen, H.; Chakrabarti, A. *J. Chem. Phys.* **1998**, *108*, 6897.
- [19] Onuki, A.; Fukuda, J. *Macromolecules* **1995**, *28*, 8788.
- [20] Pereira, G. G.; Williams, D. R. M. *Macromolecules* **1999**, *32*, 8115.
- [21] de Gennes, P. G.; Prost, J. *The Physics of Liquid Crystals*, Oxford University: New York, 1993. Helfrich, W. *Appl. Phys. Lett.* **1970**, *17*, 531. Helfrich, W. *J. Chem. Phys.* **1971**, *55*, 839. Hurault, J. P. *J. Chem. Phys.* **1973**, *59*, 2068.
- [22] Ashok, B.; Muthukumar, M.; Russell, T. P. *J. Chem. Phys.* **2001**, *115*, 1559.

- [23] Brazovskii, S. A. *Sov. Phys. JETP* **1975**, *41*, 85.
- [24] Fabre, P.; Casagrande, C.; Veyssie, M.; Cabuil, V.; Massart, R. *Phys. Rev. Lett.* **1990**, *64*, 539.

- **Figure 1:** Schematic illustration of the system. The two confining surfaces are at  $y = \pm \frac{1}{2}L$ , and have interaction parameters  $\sigma^\pm$ . The electric field points in the perpendicular  $y$  direction, and is produced by a potential difference between the two surfaces (electrodes).
- **Figure 2:** Weight functions  $w(E)$  and  $g(E)$ . The horizontal dash-dot line  $w = 1/\sqrt{2}$  is the value of  $w$  below which a nonzero  $g(E)$  is possible. Surface separation is  $L = 8d_0$  and the Flory parameter is  $N\chi = 11$ . The film is symmetric,  $\sigma^+ = \sigma^- = 0.6hq_0^3\phi_L$ .
- **Figure 3:** (a) Critical field  $E_c$  [in units of  $(hq_0^4/\beta)^{1/2}$ ] required for the appearance of perpendicular lamellae, as a function of surface separation  $L$ . (b) log-log plot of the same curve as in part a. The dashed line is a fit to a  $L^{-1/2}$  behavior. (c) The jumps  $\Delta g$  (dashed line) and  $\Delta w$  (solid) in the amplitudes  $g$  and  $w$  at the critical field  $E_c$ , as a function of surface separation  $L$ . The film is symmetric, and  $\sigma^\pm$  and  $N\chi$  are as in Fig. 2.
- **Figure 4:** Contour plots of the BCP order parameter  $\phi(x, y) = w(E)\phi_\parallel(y) + g(E)\phi_\perp(x)$  for symmetric film. The surfaces are at  $y = \pm L = \pm 2d_0$ , and the field is in the  $y$  direction. In part a the field is a little smaller than the critical field,  $E = 0.98E_c$ , and the film has a perfect parallel ordering. In part b the field is just above the threshold,  $E = 1.02E_c$ . The film morphology is a superposition of parallel and perpendicular lamellae. (c) A plot of the IMDS [given by  $\phi(x, y) = 0$ ] of part b. In (d)  $E = 4E_c$ , and the lamellae are in the perpendicular state with small distortions. The surface fields are  $\sigma^+ = \sigma^- = 0.5hq_0^3\phi_L$ , and the Flory parameter is  $N\chi = 11$ . The B monomers (colored black) are attracted to the two symmetric surfaces.
- **Figure 5:** Illustration of the lamellae in the film in the strong segregation regime. A region with perpendicular lamellae exists in the middle of the film, with size  $l$ .
- **Figure 6:** (a) Qualitative dependence of  $\gamma_T$  and  $\sigma_{BS}$  on the thickness of perpendicular domain  $\ell$ , defined in Fig. 5. b Simplified curves of part a. The cutoff width is  $a$ , the film thickness is  $L$ , and  $\gamma_T^0$  and  $\sigma_{BS}^0$  are the mean values of  $\gamma_T$  and  $\sigma_{BS}$ , respectively, for  $a < \ell < L - a$ .

- **Figure 7:** Sketch of the dependence of  $F_{\parallel}$ ,  $F_{\perp}$  and  $F_M$  on the field  $E$ , in solid line, circles and dashed line, respectively. (a)  $\delta > \delta^*$ : There are two critical fields, obtained when  $F_M(E) = F_{\parallel}(E)$  and  $F_{\perp}(E) = F_{\parallel}(E)$ . (b)  $\delta < \delta^*$ :  $F_M(E)$  is always larger than  $F_{\perp}(E)$ , and there is only one critical field obtained when  $F_{\parallel}(E) = F_{\perp}(E)$ . Above this field the most stable state is the perpendicular ordering.
- **Figure 8:** (a) Phase diagram in the  $E$ - $\delta$  plane. If  $\delta = (\sigma_{AS} - \sigma_{BS})/\gamma_T < \delta^*$ , there is a transition between parallel and perpendicular lamellae at  $E = E_1$ . For  $\delta > \delta^*$ , there is one transition to the mixed state, accompanied by a second transition to the perpendicular state when  $E = E_2$ . Surface separation is chosen as  $L = 10d_0$  and  $a = d_0$ . (b) Similar diagram, but in the  $E$ - $L$  plane, with  $\delta = 5$ . In both parts, the effect of mismatch between  $L$  and  $d_0$  is neglected, and the electric fields are scaled by  $[\gamma_T/d_0(\lambda_{\perp} - \lambda_{\parallel})]^{1/2}$ .
- **Figure 9:** Phase diagrams as in Fig. 8, but for strained films. The critical field  $E_1$  has oscillations as a function of  $L$ , compare to Fig. 8 b.

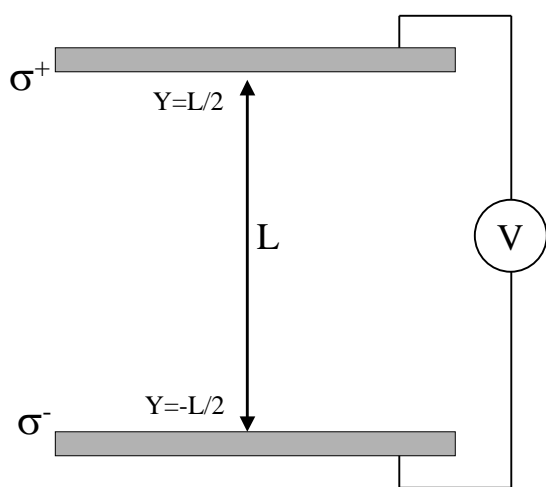


Fig. 1  
Tsori + Andelman

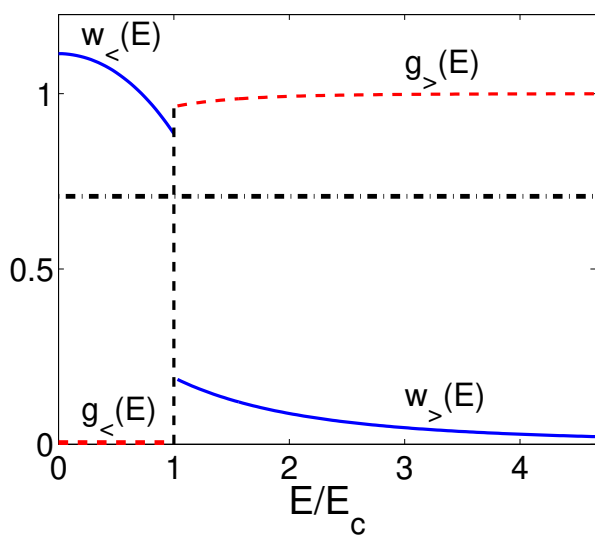


Fig. 2  
Tsori + Andelman

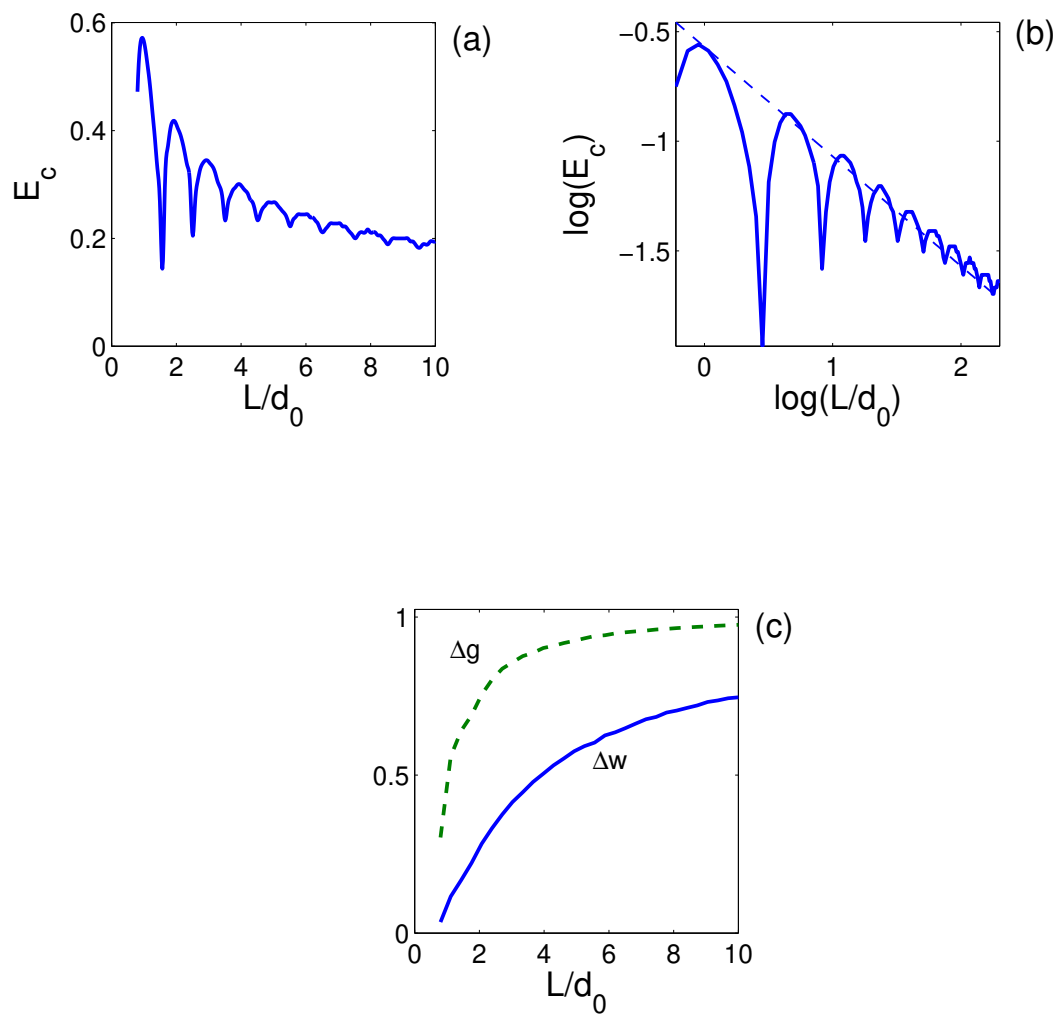


Fig. 3  
Tsori + Andelman



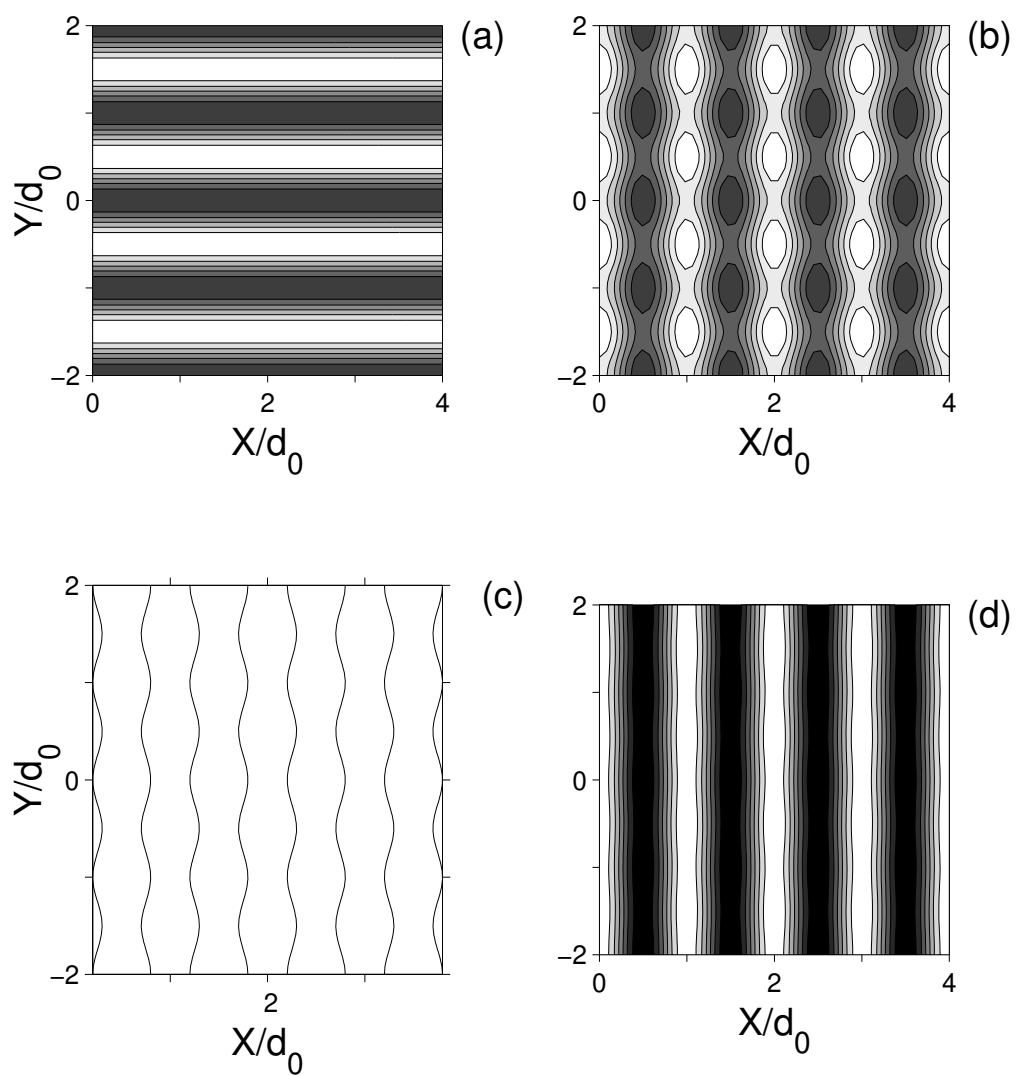


Fig. 4  
Tsori + Andelman

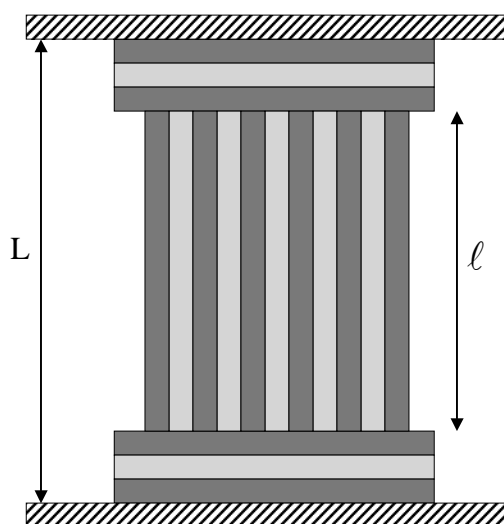


Fig. 5  
Tsori + Andelman

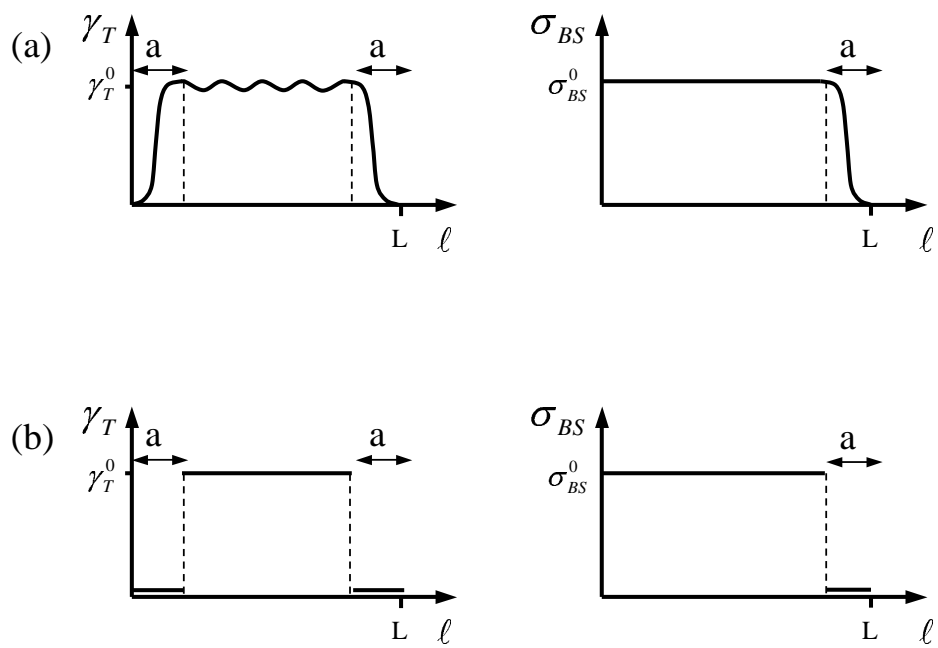


Fig. 6  
Tsori + Andelman

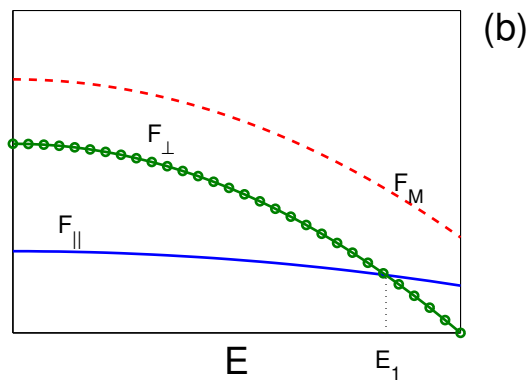
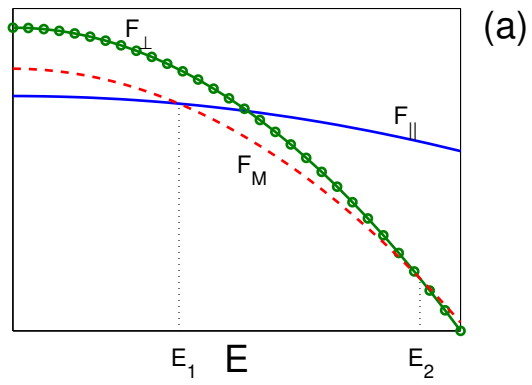


Fig. 7  
Tsori + Andelman

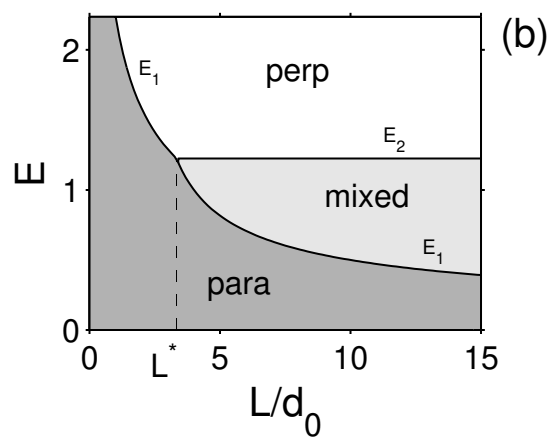
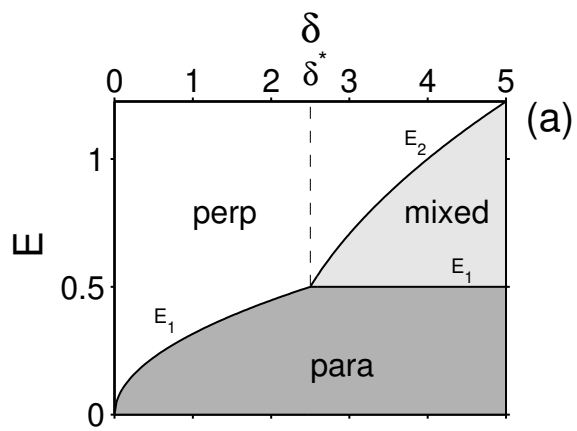


Fig. 8  
Tsori + Andelman

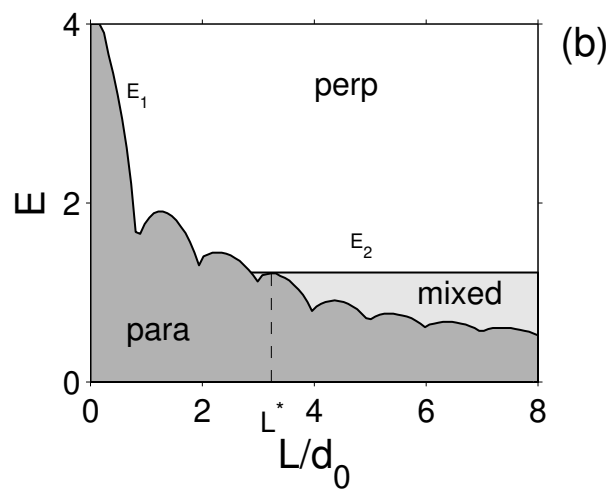
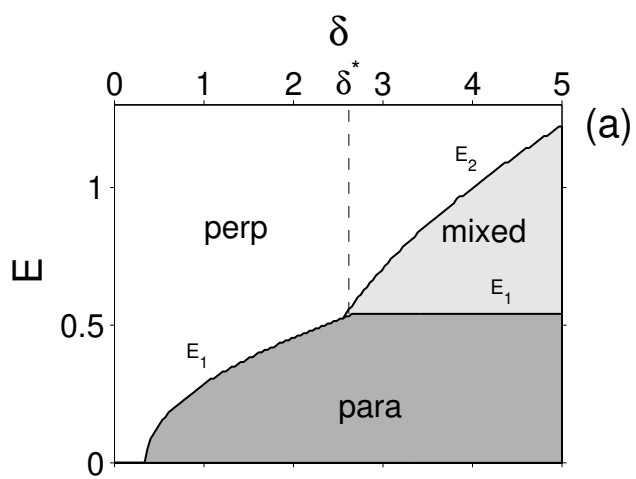


Fig. 9  
Tsori + Andelman